proceedings

MDPI

Conference Proceedings Paper

On Spacetime Duality and Bounce Cosmology of a Dual Universe

Mohammed B. Al-Fadhli [1,*]

[1] College of Science, University of Lincoln, Lincoln, LN6 7TS, UK.
* Correspondance: malfadhli@lincoln.ac.uk; mo.fadhli7@gmail.com.

Abstract: The recent Planck Legacy (PL18) release revealed the presence of an enhanced lensing amplitude in the cosmic microwave background (CMB). Notably, this amplitude is higher than that estimated by the lambda cold dark matter model (ΛCDM), which endorses a positively curved early Universe with a confidence level greater than 99%. In this study, quantised spacetime worldlines are utilised to model the evolution of the Universe with reference to the scale factor of the early Universe and its radius of curvature. The worldlines revealed both positive and negative solutions, implying that matter and antimatter of early Universe plasma evolved in opposite directions as distinct Universe sides during a first decelerating phase, corroborating the CMB dipole anisotropy. The worldlines then indicated a second accelerated phase in reverse directions, where both sides could be free-falling towards each other under gravitational acceleration. Simulations of the spacetime continuum flux through its travel along the predicted worldlines demonstrated the fast-orbital speed of stars resulting from external fields exerted on galaxies via the spatial curvature through the imaginary time dimension. Finally, the worldlines predicted a final time-reversal phase of rapid spatial contraction leading to a Big Crunch, signalling a cyclic Universe. These findings indicate that early Universe plasma could be separated and evolved into distinct Universe sides that collectively and geometrically influencing the evolution of the Universe, physically explaining the effects attributed to dark matter and dark energy.

Keywords: accelerated expansion; duality; antimatter

1. Introduction

Bounce cosmology provides an alternative perception of the Universe, in which our Universe expanded from a hot and very dense state of a previously collapsed Universe [1]. The idea was first proposed by Tolman in the 1930s; since then, many bouncing models have been introduced with the aim of providing a systematic description of the beginning and evolution of the Universe [2].

This cosmology is free from the singularity problem and offers a clearer view of the early Universe [2]. However, the null-energy condition is generally violated by the conjectured bounce of re-expansion in several modified gravity theories [3,4]. Alternatively, the bounce realisation could be sought through other scenarios, such as the phenomenon of plasma drift in the presence of electromagnetic fields [5,6]. In this sense, matter and antimatter of early Universe plasma could have been separated upon the emission of the CMB and consequently evolved in opposite directions due to their opposite spin and charge. Additionally, in realising the singularity-free paradigm, a minimal Universe's radius can be sought by considering the boundary contribution and the pre-existing curvature of early Universe plasma based on the release Planck Legacy that indicated a positively curved early Universe with a confidence level higher than 99% [7].

A closed early Universe model is considered according to the PL18 recent release, where a solely theoretical work corroborated by mathematical proofs is presented in this study. The evolution of the Universe from early Universe plasma is modelled by utilising

quantised spacetime continuum worldlines. The paper is organised as follows. Section 2 introduces the extended field equations considering the background/pre-existing curvature. Sections 3 and 4 discuss the derivation of the quantised worldlines and the evolution of the Universe, while Section 5 illustrates the spiral galaxy rotation under external fields. Section 6 discusses the early Universe boundary contribution and the minimal Universe radius. Finally, Section 7 concludes this work and suggests future works.

2. Extended Field Equations for a Curved Early Universe

In addition to the PL18 evidence of a curved early Universe, recent findings regarding light polarisation from the CMB support the concept of an exotic substance through space causing these measured polarisations [8]. Accordingly, spacetime is regarded in this study as a continuum with a dual quantum nature such that it curves according to the General Relativity as waves and fluxes as quantum energy particles. The latter is justified by the energy flux from early Universe plasma into space at the speed of light creating a 'spacetime continuum' or 'vacuum energy' whereas the Universe expands. A modulus of spacetime continuum's deformation/curvature E_D is defined to incorporate the pre-existing/background curvature signified by the scalar curvature $\mathcal{R}$ into the Einstein–Hilbert action. By using the Einstein field equations, E_D =(stress/strain) is expressed as

$$E_D = \frac{T_\mu^v - T\delta_\mu^v/2}{R_\mu^v/\mathcal{R}} \tag{1}$$

where the stress is signified by the stress-energy tensor T_ν^μ of trace T, while the strain is signified by the Ricci curvature tensor R_ν^μ as the change in the curvature divided by the pre-existing curvature $\mathcal{R}$, while δ_u^v is the Kronecker delta [9]. According to the Theory of Elasticity, the modulus times the volume equals the internal energy of reversible systems [10]. Thus, E_D could represent the internal energy density of the space, i.e. the vacuum energy density. In addition, according to Eq. (1), $E_D = \mathcal{R}c^4/8\pi G$, which is proportional to the fourth-order of the speed of light c, in accordance with Quantum Field Theory energy cut-off predictions of vacuum energy density [11]. By complying with the energy conservation law, the Einstein–Hilbert action can be extended to

$$S = \int \left[\frac{E_D}{2}\frac{R}{\mathcal{R}} + \mathcal{L}\right]\sqrt{-g}\, d^4x \tag{2}$$

where $\mathcal{L}$ is the Lagrangian density, R is the Ricci scalar curvature and g is the determinant of the metric tensor g_{uv}. The derivations of the extended action in Ref. [12] as

$$\frac{R_{\mu\nu}}{\mathcal{R}} - \frac{1}{2}\frac{R}{\mathcal{R}}\hat{g}_{\mu\nu} + \frac{R-\mathcal{R}}{\mathcal{R}^2}(K_{\mu\nu} - \frac{1}{2}K\hat{q}_{\mu\nu}) = \frac{T_{\mu\nu}}{E_D} \tag{3}$$

Eqs. (3) can be interpreted as indicating that the induced curvature over the pre-existing curvature equals the ratio of the imposed energy density, and its flux, to the vacuum energy density and its flux through an expanding/contracting Universe. Here, $\hat{g}_{\mu\nu} = g_{\mu\nu} + 2\bar{g}_{\mu\nu}$ denotes the conformal transformation of the metric because Einstein spaces are a subclass of the conformal space [13]. The conformal transformation could describe the tidal distortion and gravitational waves in the absence of matter [14]. $K_{\mu\nu}$ is the extrinsic curvature tensor and $\hat{q}_{\mu\nu}$ is the conformally transformed induced metric on the spacetime manifold boundary. The extended field equations can be simplified by substituting E_D value in Eqs. (3) as

$$R_{\mu\nu} - \frac{1}{2}R\hat{g}_{\mu\nu} + \frac{R-\mathcal{R}}{\mathcal{R}}(K_{\mu\nu} - \frac{1}{2}K\hat{q}_{\mu\nu}) = \frac{8\pi G}{c^4}T_{\mu\nu} \tag{4}$$

The new boundary term/tensor is only significant at high-energy limits such as within black holes [15] and the early Universe where it could remove the singularities from the theory.

3. Bounce from a Closed Early Universe

The Friedmann–Lemaîtree–Robertson–Walker (FLRW) metric is the standard cosmological metric model, which assumes an isotropic and homogenous Universe [16,17], where the isotropy and homogeneity of the early Universe plasma based on the CMB are consistent with this model. The PL18 release revealed a closed and positively curved early Universe. Accordingly, the plasma reference radius of curvature r_P upon the emission of the CMB and the corresponding early Universe scale factor a_P at reference time t_p are incorporated to reference the FLRW metric model as shown in Figure 1.

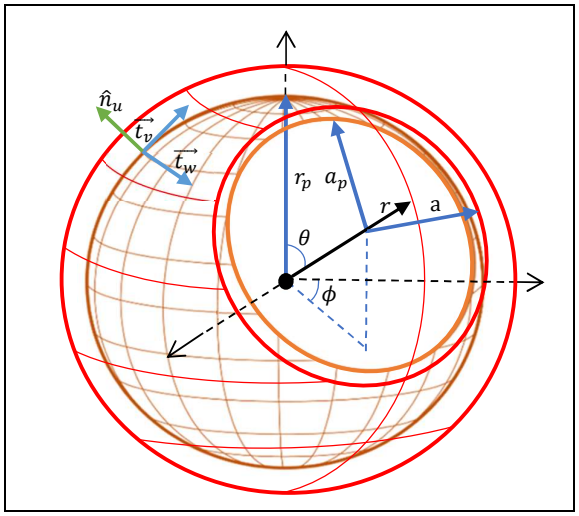

Figure 1. The hypersphere of a positively curved early Universe plasma expansion upon the CMB emissions. r_p is the reference radius of the intrinsic curvature and a_p is the reference scale factor of the early Universe at the corresponding reference time t_p. $\hat{n}_u$ and $\vec{t}_{v,w}$ are the normal and tangential vectors on the manifold boundary respectively regarding the extrinsic curvature. r, ϕ, θ are the comoving coordinates.

The referenced metric tensor is

$$[g_{\mu\nu}(\mathrm{x})] = \mathrm{diag}\left(-c^2, \frac{a^2(t)}{{a_p}^2}/\left(1-\frac{r^2}{{r_p}^2}\right), \frac{a^2(t)}{{a_p}^2}r^2, \frac{a^2(t)}{{a_p}^2}r^2 sin^2\theta\right), \tag{5}$$

where $a\,(t)/a_p$ is a new dimensionless scale factor and r, ϕ, θ are the comoving coordinates. No conformal transformation is included in this metric, therefore, its outcomes are comparable with the literature. The Ricci curvature tensor R_{uv} is solved using Christoffel symbols for g_{uv} in Eqs. (5) as follows

$$\begin{aligned} R_{tt} &= -3\frac{\ddot{a}}{a}, \qquad R_{rr} = \frac{1}{c^2}\left(\frac{a\ddot{a}}{{a_p}^2}+\frac{2\dot{a}^2}{{a_p}^2}+\frac{2c^2}{{r_p}^2}\right)/\left(1-\frac{r^2}{{r_p}^2}\right), \\ R_{\theta\theta} &= \frac{r^2}{c^2}\left(\frac{a\ddot{a}}{{a_p}^2}+\frac{2\dot{a}^2}{{a_p}^2}+\frac{2c^2}{{r_p}^2}\right), \qquad R_{\phi\phi} = \frac{r^2 sin^2\theta}{c^2}\left(\frac{a\ddot{a}}{{a_p}^2}+\frac{2\dot{a}^2}{{a_p}^2}+\frac{2c^2}{{r_p}^2}\right), \end{aligned} \tag{6}$$

The Ricci scalar curvature is

$$R = R_{\mu\nu}\, g^{\mu\nu} = -\frac{6}{c^2}\left(\frac{\ddot{a}}{a}+\frac{\dot{a}^2}{a^2}+\frac{c^2\,{a_p}^2}{a^2\,{r_p}^2}\right). \tag{7}$$

where $\ddot{a}$ and $\dot{a}$ are the second and the first derivatives of a respectively.

By using Eqs. (5-7) that count for the plasma parameters and considering a perfect fluid given by $T_{\mu\nu} = (\rho + \frac{P}{c^2})\, u_\mu u_\nu + P g_{\mu\nu}$ [9] in solving Einstein field equations results in

the referenced Friedmann equations:

$$H^2 \equiv \frac{\dot{a}^2}{a^2} = \frac{8\pi G\,\rho}{3} - \frac{c^2\,a_p{}^2}{a^2\,r_p{}^2}, \tag{8}$$

$$\dot{H} \equiv \frac{\ddot{a}}{a} = -\frac{4\pi G}{3}\left(\rho + 3\frac{P}{c^2}\right). \tag{9}$$

where H, P, and ρ are the Hubble parameter, pressure, and density respectively.

By utilising the imaginary time, the referenced Friedman equations in Eqs. (8, 9) are solved over the conformal time by rewriting Eq. (8) in terms of the conformal time in its parametric form $d\eta = -i\frac{a_p}{a}d\tau$ while initiating at the reference imaginary time τ_p as

$$\int_0^{\eta} d\eta = \int_0^{2\pi} a_p \left(\frac{8\pi G\,\rho_p a_p{}^3}{3}a - \frac{c^2 a_p{}^2}{r_p{}^2}a^2\right)^{-1/2} da \tag{10}$$

where $\rho = \frac{\rho_p a_p{}^3}{a^3}$ [18]. By integrating, the scale factor evolution is

$$a(\eta)/a_p = \frac{M_p G}{c^2 r_p}\left(1 - cos\frac{c}{r_p}\eta\right) \tag{11}$$

where $M_p = \frac{4}{3}\pi\rho_p r_p{}^3$ is the plasma mass at τ_p. The constant in Eq. (11) can be written in terms of the modulus E_D representing the vacuum energy density and the Universe energy density E using Eq. (1) as $E/6E_D$.

Additionally, the evolution of the imaginary time $\tau(\eta)$ can be obtained by integrating the length of the spatial factor contour of one Universe life cycle over the expansion speed H_η while initiating at the reference imaginary time τ_p with the corresponding spatial factor a_p. Thus, by rewriting Eq. (9) in terms of the Hubble parameter by its definition at τ_p as $d\tau = i\frac{da}{Ha_p}$ as

$$\int_{\tau_P}^{\tau} d\tau = i\int_0^{\eta} \frac{E}{6H_\eta E_D}\left(1 - cos\frac{c}{r_p}\eta\right)d\eta \tag{12}$$

By performing the integration, the imaginary time evolution is

$$\tau(\eta) = i\frac{E}{6H_\eta E_D}\left(\eta - \sin\frac{c}{r_0}\eta\right) + \tau_p \tag{13}$$

According to the law of energy conservation, the covariant divergence of the stress-energy tensor vanishes, $\Delta_v T^{uv} = 0$, this yields $\frac{\dot{a}}{a}T_u^u + 3\frac{\dot{a}}{a}\rho - i\frac{\partial\rho}{\partial\tau} = 0$, $3\left(\rho + \frac{P}{c^2}\right)\frac{\dot{a}}{a} - i\frac{\partial\rho}{\partial\tau} = 0$. By combining these outcomes, integrating, and substituting the spatial scale factor rate in Eq. (11) to their outcome, the Universe density evolution over the conformal time is

$$\rho_\eta = D_p\left(1 - cos\frac{c}{r_p}\eta\right)^{-3} \tag{14}$$

where D_P is a constant. By substituting Eq. (14) in Eq. (9) and initiating the integration at τ_p thus, $\dot{H} = \frac{\ddot{a}}{a_p}$ as

$$\int_{H_p}^{H} \dot{H} = \int_0^{\eta} -\frac{4\pi G\,D_p}{3a_p}\left(1 - \cos\frac{c}{r_p}\eta\right)^{-3} d\eta \tag{15}$$

By integration, the Hubble parameter evolution is

$$H_\eta = H_a\left(\frac{1}{5}\cot^5\frac{c}{2r_p}\eta + \frac{2}{3}\cot^3\frac{c}{2r_p}\eta + \cot\frac{c}{2r_p}\eta\right) + H_p \tag{16}$$

where H_a and H_p are constants.

The quantised hyperspherical spacetime wave function $\overrightarrow{\psi_L}(\eta)$ with respect to the reference wave function ψ_p at τ_p is obtained using Eqs. (11, 13-16) as a possible third quantisation:

$$\overrightarrow{\psi_L}(\eta)/\psi_p = \mp\frac{E}{6E_D}\left(\left(\left(1-\cos\frac{c}{r_p}\eta\right)^2 + \frac{c^2}{H_\eta{}^2 a_p^2}\left(\eta-\sin\frac{c}{r_p}\eta\right)^2\right)^{1/2}\right) e^{i\cot\frac{H_\eta a_p\left(1-cos\frac{c}{r_p}\eta\right)}{c\left(\eta-sin\frac{c}{r_p}\eta\right)}} \quad (17)$$

where E/E_D denotes a new dimensionless energy density parameter as the ratio of the Universe energy density to the vacuum energy density.

4. Evolution of Universe Worldlines

The positive and negative solutions of the wave function in Eq. (17) imply that matter and antimatter in the plasma evolved in opposite directions. The phenomenon of plasma drift is caused by the presence of electromagnetic fields [5,6], which drives matter and antimatter in opposite directions, as they have opposite electrical charges. A chosen mean evolution value of the Hubble parameter of ~70 km·s-1·Mpc-1 and a phase transition of expansion at Universe's age of ~10 Gyr were applied to tune the integration constants of the derived model, where the predicted energy density parameter is ~1.16.

The cosmic evolution of radiation coupled with matter/antimatter according to the wave function is predicted to experience three distinct phases (Figure 2a, orange curve) while radiation only worldlines, which propagate faster than matter/antimatter, is predicted to pass to the other side (blue curve). Due to symmetry, only the positive solution is shown in Figure 2a. Additionally, the predicted Hubble parameter H (speed of the spatial expansion) and its rate $\dot{H}$ (the spatial expansion acceleration) along with a rectified Hubble parameter reflecting the reverse evolution, direction are shown in Figure 2b.

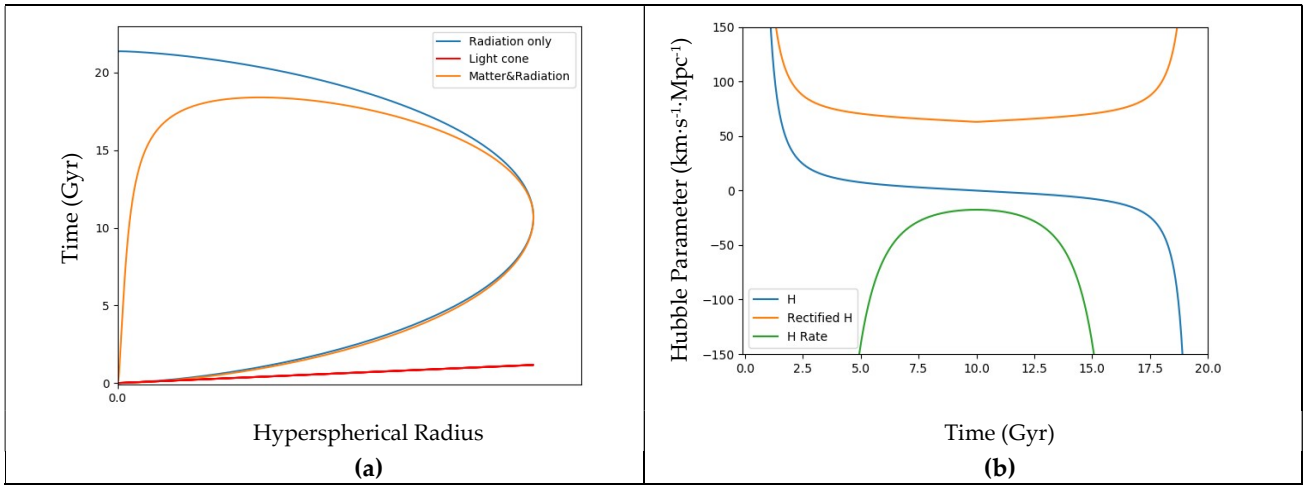

Figure 2. (**a**) Evolution of the wave function of matter coupled with radiation of one side of the Universe, radiation only wave function in addition to the straight line of light cone (diagram is not to scale). (**b**) The Hubble parameter H evolution and its rate. The orange curve shows a deceleration during the first ~10 Gyr followed by an accelerated expansion rate.

These results can be interpreted as follows. Firstly, the matter and antimatter sides expanded in opposite directions away from the early Universe plasma, possibly due to the phenomenon of plasma drift, where they would be blue and red-shifted in corresponding the CMB dipole anisotropy. During the first phase (i.e., the first ~10 Gyr), the expansion rate or the Hubble parameter shown in Figure 2b (blue curve) starts with a hyperbolic

expansion rate at the nascent stage upon the emission of CMB where the expansion rate is at its highest value. Then, the rate decreases, which could be due to gravity between both sides, until it reaches its minimal value at the phase transition.

However, at the second phase, the worldlines reverse their directions, with both sides of the matter and antimatter entering a state of free fall towards each other under gravitational acceleration causing current accelerated expansion, while vacuum energy cannot be responsible for this acceleration [19]. The Hubble parameter starts to increase in the second phase. According to the mechanics, the minus sign of the Hubble parameter (the speed of expansion) indicates an opposite expansion direction. Further, the opposite signs of the acceleration (green curve) and the expansion speed in the first phase indicate a slowing down while the matching signs in the second phase indicate the expansion speed is increasing. Interestingly, the model predicts a third phase of spatial contraction that appears after ~ 18 Gyr, where the Universe experiences a contraction, which could be due to a high concentration of matter/antimatter at both sides, leading to the big Crunch.

Parallel worldlines were simulated according to the model in Eq. (17), where they produced a flat end or flat spacetime at the second phase of reverse directions as shown in Figure 3a, a schematic of 2D spatial and 1D temporal dimensions. The radiation only worldlines is predicted to pass from one side to another, which could explain why CMB light can be observed even though matter moves much more slowly than light. Additionally, Figure 3b shows an approximate apparent topology due to gravitational lensing effects, which possibly in accordance with the large-angle correlations of the CMB and the SLOAN Digital Sky Survey data.

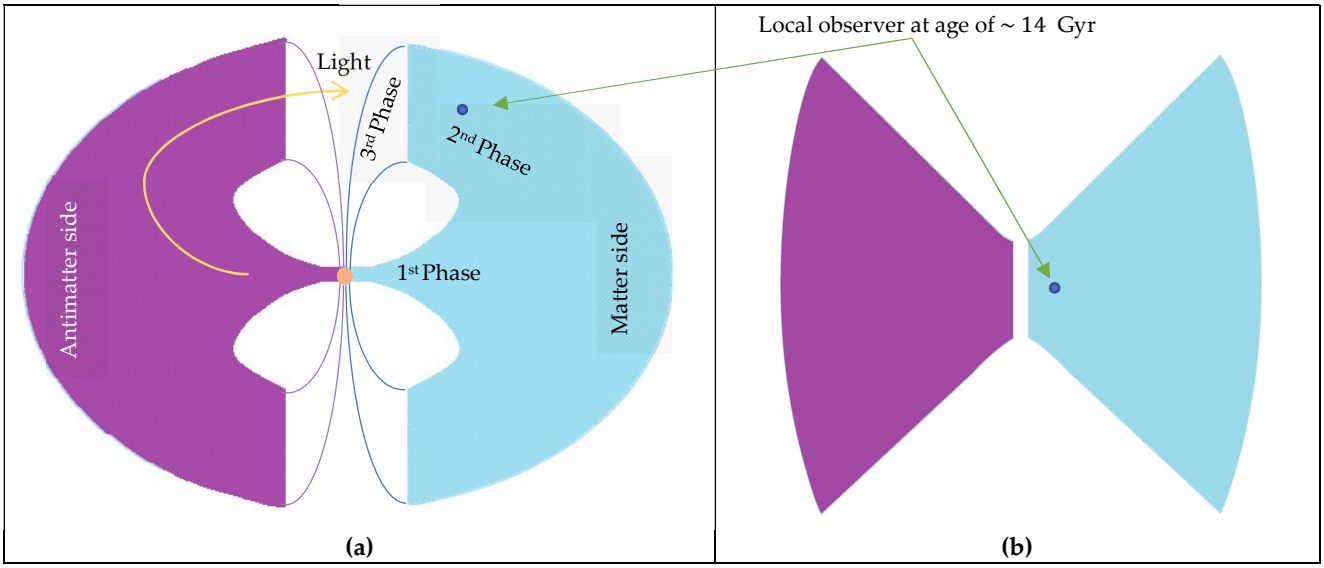

Figure 3. (**a**) 2D-schematic of the predicted cosmic topology of both sides at the first phase away from the early plasma while the second phase corresponding to the reversal of the expansion direction. The future third phase corresponds to a spatial contraction leading to a Big Crunch. (**b**) The apparent topology during the first and second phases caused by gravitational lensing effects.

A 3D spatial and 1D temporal dimensions schematic of the spacetime evolutions of both sides is shown in Figure 4, where antimatter travels backwards in time. As at the second phase, both sides move closer to each other, this could explain the current increase in the average temperature of the Universe [20], in contrast to the state of cooling down from the hot plasma during the first phase.

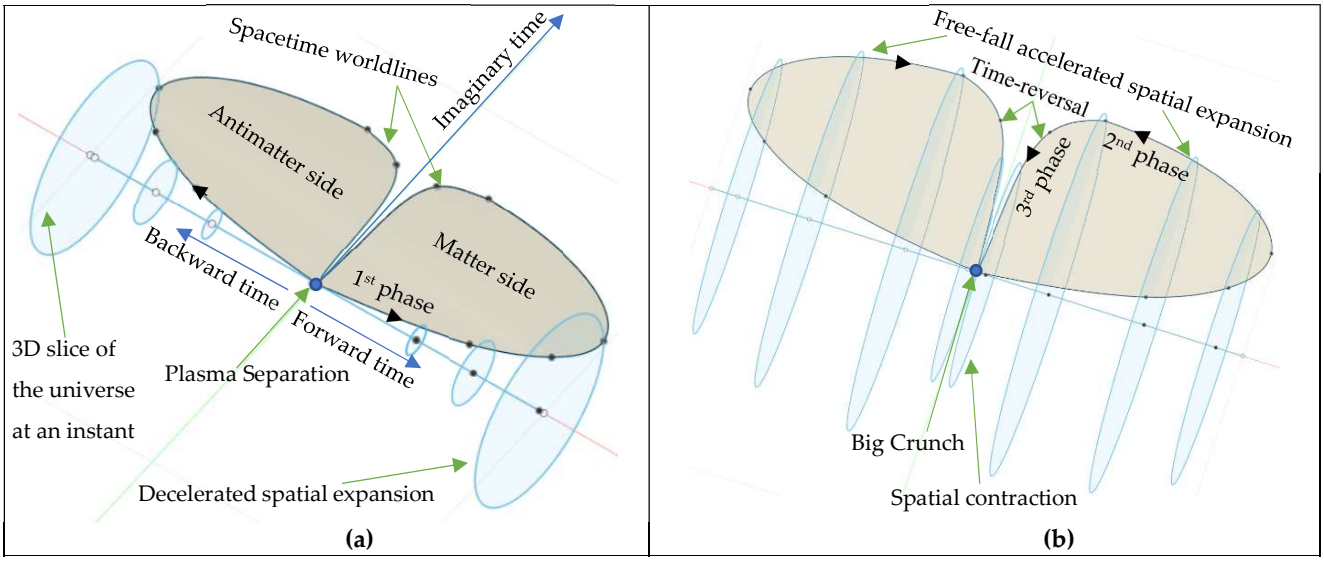

Figure 4. Schematic in 3D spatial and 1D temporal dimensions of both sides, according to the wave function of spacetime worldlines. (**a**) In the first phase, both sides expand away from the early plasma. **(b)** In the second stage, both sides expand in reverse directions and free-fall towards each other at gravitational acceleration. In the third phase, both sides contract leading to the big Crunch. Blue circles represent a 3D slice of the Universe that is not necessarily a simply path connected.

5. Spiral Galaxy Rotation under External Fields

The derived model in Eq. (17) predicted that the curvature of the spacetime continuum increases along with its worldline evolution, with the highest degree of curvature occurring at the phase transition, as shown in Figures 2a and 3a. It can be inferred the fast-orbital speeds observed for outer stars are a result of the variation of spacetime continuum curvature, which can exert external fields on galaxies. To evaluate this, a fluid simulation study was performed using the Fluid, Pressure and Flow software [21] as in Figure 5a.

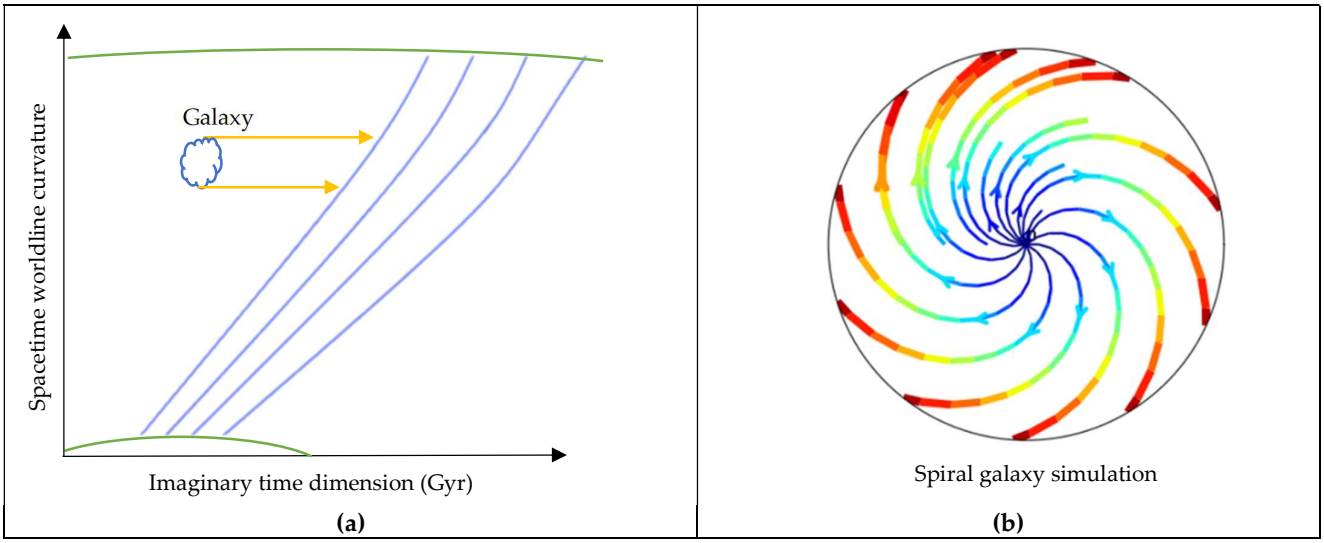

Figure 5. (**a**) External fields exerted on a galaxy because of the divergence of spatial curvature through the imaginary time dimension. Green curves represent the curvature of spacetime worldlines. Blue curves represent the simulated spacetime continuum flux. (**b**) Spiral galaxy rotation. Blue represents the slowest tangential speeds, and red represents the fastest speeds.

In this simulation, the fluid flow was utilised to simulate the spacetime continuum flux through incrementally flatter worldline curvature. Using the resultant momentums on objects flowing inside the fluid, a simulation of a spiral galaxy as a forced vortex was created as shown in Figure 5b.

The simulation shows that the tangential speeds of outer parts of the spiral galaxy are rotating faster in comparison with the rotational speeds of inner parts. Additionally, galaxies of the same mass in the present Universe are rotating faster than they were in the past because of the increase in the external fields due to the highest spatial curvature at the phase transition, which could agree with the Tully–Fisher relation [22]. Based on the simulation results, it can be concluded the spacetime continuum curvature along its worldline evolution is responsible for the high speed of galaxies, explaining the effects attributed to dark matter. In contrast with the dark matter hypothesis as particles which is being challenged by findings of external fields reported in Ref. [23] or MOND which is being challenged by gravitational lensing as well as its prediction of the slower speed of gravitational waves than the speed of light [24].

6. Early Universe Boundary Contribution

At high energy limits, gravitational contributions of early Universe plasma boundary can be obtained using the boundary term/tensor in the extended field equations $\frac{R-\mathcal{R}}{\mathcal{R}}\left(K_{\mu\nu}-\frac{1}{2}K\hat{q}_{\mu\nu}\right)=\frac{8\pi G}{c^4}T_{\mu\nu}$. At the reference imaginary time τ_p, there is no conformal transformation. Therefore, the induced metric tensor $q_{\mu\nu}$ on early Universe plasma hypersphere is given in Eqs. (18), where R is the extrinsic radius of curvature [25]:

$$\left[q_{\mu\nu}(\mathrm{x})\right]=\mathrm{diag}\left(-c^2,\frac{a^2(t)}{{a_p}^2}R^2,\frac{a^2(t)}{{a_p}^2}R^2sin^2\theta\right), \tag{18}$$

The extrinsic curvature tensor is solved by utilising the formula $K_{uv}=-\overrightarrow{t_v}.\nabla_u\hat{n}_u$. Due to the smoothness of the hypersphere, the covariant derivative reduces to the partial derivative as $K_{uv}=-\overrightarrow{t_v}\,\partial\hat{n}_u/\partial\overrightarrow{t^u}$ [25]. The extrinsic curvature tensor at τ_p is

$$[K_{\mu\nu}(\mathrm{x})]=\mathrm{diag}\left(0,-\frac{a^2(t)}{{a_p}^2}R,-\frac{a^2(t)}{{a_p}^2}Rsin^2\theta\right) \tag{19}$$

The trace of the extrinsic curvature is $K=K_{\mu\nu}q^{\mu\nu}=2/R$. The pre-existing/intrinsic curvature of early Universe plasma boundary at τ_p is the Gaussian curvature $\mathcal{R}_p=1/r_p^2$ [25].

On the other hand, the Ricci scalar curvature R_p at τ_p can be written in terms of the difference between kinetic and potential energy densities whereby substituting Friedmann equations in Eqs. (8, 9) into the Ricci scalar curvature in Eq. (7) as

$$R_p=\frac{6G}{c^2}\left(\frac{4\pi P_p}{c^2}-\frac{4\pi\rho_p}{3}\right) \tag{20}$$

By solving the boundary term $\frac{R-\mathcal{R}}{\mathcal{R}}(K_{\mu\nu}-\frac{1}{2}Kq_{\mu\nu})=\frac{8\pi G}{c^4}T_{\mu\nu}$ for a perfect fluid given by $T_{\mu\nu}=(\rho+\frac{P}{c^2})\,u_\mu u_\nu+Pg_{\mu\nu}$ [9], and then substituting Eqs. (18-19) into the boundary term:

$$\frac{\frac{6G}{c^2}\left(\frac{4\pi P_p}{c^2}-\frac{4\pi\rho_p}{3}\right)-\frac{1}{r_p^2}}{1/r_p^2}\left(\frac{-c^2}{r_p^2}\right)=8\pi G_p\rho_p \tag{21}$$

Multiplying by early Universe plasma volume V_p yields

$$r_p=\frac{4G\,P_pV_p}{c^4}=\sqrt[3]{\frac{E_p}{2\pi E_D}} \tag{22}$$

where E_p is the early Universe plasma energy. The reference radius of curvature $r_p>0$ because any reduction in the volume causes an increase in the pressure, which can realise a singularity-free paradigm.

7. Conclusions and Future Works

In this study, a closed early Universe model was considered by utilising the referenced FLRW metric model. The evolution of the Universe from early plasma was modelled utilising quantised spacetime continuum worldlines. The worldlines revealed two opposite solutions implying that the Universe into two sides: matter and antimatter.

The derived model predicted that a nascent hyperbolic expansion is followed by a phase of decelerating spatial expansion during the first ~ 10 Gyr, followed by a second phase of accelerating expansion, theoretically resolving the tension in Hubble parameter measurements. Both sides of the Universe expand away from the early plasma during the first phase. Then, during the second phase, they reverse their directions and fall towards each other. It is conceivable that the matter and antimatter are free-falling towards, causing the current accelerating expansion of the Universe. This could explain the effects attributed to dark energy as well as the observed dark flow.

Further, the simulated spacetime worldlines during the decelerating phase were found to be flattened during the accelerating phase due to the reverse direction of the continuum worldlines, explaining the current space flatness. Regarding the fast-orbital speed of stars, the simulation could provide a physical explanation by which the spatial curvature through the imaginary time dimension along with the spacetime continuum worldlines of both sides was found to exert external fields on galaxies. Thus, the geometrical spacetime curvature can be causing them to increase in speed, rather than the existence of dark matter.

The model predicted a final phase of time-reversal of spatial contraction leading to a Big Crunch, signifying a cyclic Universe. The derived smallest possible reference radius of the early plasma due to its boundary gravitational contributions can reveal the early Universe expansion upon emission of the CMB might mark the beginning of the Universe from a previous collapse one. Finally, this theoretical work will be tested against observational data in future works.

Acknowledgements: I would express my gratitude to the Preprints Editors Ms Mila Marinkovic and Ms Bojana Djokic for their rapid and excellent processing of a series of preprints during this work development.

Funding: This research received no funding.

Conflicts of Interest: The author declares no conflict of interest.

References

[1] R. C. Tolman, "On the theoretical requirements for a periodic behaviour of the universe," *Phys. Rev.*, vol. 38, no. 9, pp. 1758–1771, Nov. 1931.

[2] G. Minas, E. N. Saridakis, P. C. Stavrinos, and A. Triantafyllopoulos, "Bounce cosmology in generalized modified gravities," *Universe*, vol. 5, no. 3, p. 74, Mar. 2019.

[3] T. Singh, R. Chaubey, and A. Singh, "Bounce conditions for FRW models in modified gravity theories," *Eur. Phys. J. Plus*, vol. 130, no. 2, pp. 1–9, Feb. 2015.

[4] Y. F. Cai, D. A. Easson, and R. Brandenberger, "Towards a nonsingular bouncing cosmology," *J. Cosmol. Astropart. Phys.*, vol. 2012, no. 8, p. 020, Aug. 2012.

[5] O. Klein, "Instead of cosmology," *Nature*, vol. 211, no. 5056. Nature Publishing Group, pp. 1337–1341, 1966.

[6] O. Klein, "Arguments concerning relativity and cosmology," *Science (80-.).*, vol. 171, no. 3969, pp. 339–345, Jan. 1971.

[7] E. Di Valentino, A. Melchiorri, and J. Silk, "Planck evidence for a closed Universe and a possible crisis for cosmology," *Nat. Astron.*, vol. 4, no. 2, pp. 196–203, Feb. 2020.

[8] Y. Minami and E. Komatsu, "New Extraction of the Cosmic Birefringence from the Planck 2018 Polarization Data," *Phys. Rev. Lett.*, vol. 125, no. 22, p. 221301, Nov. 2020.

[9] N. Straumann, "General Relativity (Graduate Texts in Physics)," in *Springer*, Springer, 2013.

[10] L. D. Landau, *Theory of Elasticity*. Elsevier, 1986.

[11] S. E. Rugh and H. Zinkernagel, "The Quantum Vacuum and the Cosmological Constant Problem," *Stud. Hist. Philos. Sci. Part B - Stud. Hist. Philos. Mod. Phys.*, vol. 33, no. 4, pp. 663–705, Dec. 2000.

[12] M. B. Al-Fadhli, "Extended General Relativity for a Curved Universe," *Preprints*, Jan. 2021.

[13] C. Kozameh, E. Newman, K. T.-G. relativity and gravitation, and undefined 1985, "Conformal Einstein spaces," *Springer*, 1985.

[14] R. Penrose, *The Road to Reality: A Complete Guide to the Laws of the Universe*. 2005.

[15] E. Dyer and K. Hinterbichler, "Boundary terms, variational principles, and higher derivative modified gravity," *Phys. Rev. D - Part. Fields, Gravit. Cosmol.*, vol. 79, no. 2, Jan. 2009.

[16] M. Lachì Eze-Rey and J.-P. Luminet, "COSMIC TOPOLOGY," *arXivgr-qc/9605010v2 9 Jan 2003*, 2003.

[17] G. F. R. Ellis and H. van Elst, "Cosmological models (Carg\`{e}se lectures 1998)," Dec. 1998.

[18] B. Ryden, *Introduction to Cosmology*. San Francisco, CA, USA: Addison Wesley, ISBN 0-8053-8912-1., 2006.

[19] G. Ryskin, "Vanishing vacuum energy," *Astropart. Phys.*, vol. 115, p. 102387, Feb. 2020.

[20] Y.-K. Chiang, R. Makiya, B. Ménard, and E. Komatsu, "The Cosmic Thermal History Probed by Sunyaev-Zeldovich Effect Tomography," *arXiv*, Jun. 2020.

[21] Sam Reid et al, "Fluid Pressure and Flow, PhET Interactive Simulations." University of Colorado, 2013.

[22] R. B. Tully and J. R. Fisher, "A new method of determining distances to galaxies," *Astron. Astrophys.*, vol. 54, pp. 661–673, 1977.

[23] K. H. Chae, F. Lelli, H. Desmond, S. S. McGaugh, P. Li, and J. M. Schombert, "Testing the strong equivalence principle: Detection of the external field effect in rotationally supported galaxies," *arXiv*, vol. 904, no. 1. arXiv, p. 51, 24-Sep-2020.

[24] J. D. Bekenstein, "The modified Newtonian dynamics-MOND-and its implications for new physics," *Contemp. Phys.*, vol. 47, no. 6, pp. 387–403, Jan. 2007.

[25] Pavel Grinfeld, *Introduction to Tensor Analysis and the Calculus of Moving Surfaces*. Springer, 2013.